Greater strength of selection and higher proportion of beneficial amino acid changing mutations in humans compared to mice and *Drosophila melanogaster*

Running title: Differences in adaptive evolution across species

Authors:

Ying Zhen[1,2,3*], Christian D. Huber[1], Robert W. Davies[4], Kirk E. Lohmueller[1,5*]

Affiliations:

[1]Department of Ecology and Evolutionary Biology, University of California, Los Angeles, CA 90095

[2]School of Life Sciences, Westlake University, 18 Shilongshan Road, Hangzhou 310024, Zhejiang Province, China.

[3]Institute of Biology, Westlake Institute for Advanced Study, 18 Shilongshan Road, Hangzhou 310024, Zhejiang Province, China.

[4]Genetics and Genomic Biology and The Centre for Applied Genomics, Hospital for Sick Children, Toronto, Canada.

[5]Department of Human Genetics, David Geffen School of Medicine, University of California, Los Angeles, CA 90095

* To whom correspondence should be addressed: klohmueller@ucla.edu, zhenying@westlake.edu.cn

Keywords: Adaptive evolution, beneficial mutation, distribution of fitness effects, alpha

ABSTRACT

Quantifying and comparing the amount of adaptive evolution among different species is key to understanding evolutionary processes. Previous studies have shown differences in adaptive evolution across species; however, their specific causes remain elusive. Here, we use improved modeling of weakly deleterious mutations and the demographic history of the outgroup species and ancestral population and estimate that at least 20% of nonsynonymous substitutions between humans and an outgroup species were fixed by positive selection. This estimate is much higher than previous estimates, which did not correct for the sizes of the outgroup species and ancestral population. Next, we directly estimate the proportion and selection coefficients (p^+ and s^+, respectively) of newly arising beneficial nonsynonymous mutations in humans, mice, and *Drosophila melanogaster* by examining patterns of polymorphism and divergence. We develop a novel composite likelihood framework to test whether these parameters differ across species. Overall, we reject a model with the same p^+ and s^+ of beneficial mutations across species, and estimate that humans have a higher p^+s^+ compared to *D. melanogaster* and mice. We demonstrate that this result cannot be caused by biased gene conversion or hypermutable CpG sites. In summary, we find the proportion of beneficial mutations to be higher in humans than in *D. melanogaster* or mice, suggesting that organismal complexity, which increases the number of steps required in adaptive walks, may be a key predictor of the amount of adaptive evolution within a species.

INTRODUCTION

Since the inception of molecular population genetics, there has been tremendous interest in quantifying the amount of adaptive evolution in different organisms. The neutral theory of molecular evolution postulated that beneficial mutations are rare, and that many of the substitutions between species are neutral (Kimura 1983). One early challenge to this theory originated from a comparison of polymorphisms and divergence at synonymous and nonsynonymous sites in *Drosophila* (Fay et al. 2002; Smith and Eyre-Walker 2002). Under models without positive selection, the ratio of nonsynonymous to synonymous changes should remain equal when comparing polymorphisms (*i.e.* differences within species) and divergence (*i.e.* differences between species). In contrast to this prediction, a genome-wide excess of nonsynonymous divergence between species was observed, a pattern indicative of an abundance of positive selection in *Drosophila*. More formally, Smith and Eyre-Walker (2002) proposed a statistic, α, which is the proportion of nonsynonymous substitutions between species that can be attributed to positive selection. Application of their approach in *Drosophila* has found that at least 40% of nonsynonymous substitutions have been fixed by positive selection (Smith and Eyre-Walker 2002).

Since the publication of the original study, α has been estimated from different species across the tree of life (Fay 2011). Estimates of α vary tremendously across species, tending to be higher in insects (Andolfatto 2005; Eyre-Walker and Keightley 2009), but much lower in primates and plants (Boyko et al. 2008; Eyre-Walker and Keightley 2009; Gossmann et al. 2010). In these latter species, formal tests have been unable to reject the hypothesis that α is zero (*i.e.* no positive selection; Boyko et al. 2008; Foxe et al. 2008; Eyre-Walker and Keightley 2009). It is not clear why α varies across species. One possibility is that α is higher for species

with larger population sizes, which could occur if adaptation is mutation limited. Here, species with larger population sizes would have a higher rate of beneficial mutations. The fixation probability of a given beneficial mutation also would be higher in species with larger population size, but this effect is likely to only be important for very weakly beneficial mutations. Evidence indicates that, in some cases, α is indeed correlated with population size. For example, Phifer-Rixey et al. (2012) found that estimates of α were higher for species of mice that have larger population sizes compared to species with smaller population sizes. Further, studies found a positive correlation between α and population size when comparing different species of sunflowers (Strasburg et al. 2011) and from phylogenetically diverse taxa (Gossmann et al. 2012). More recently, Galtier (2016) found a positive correlation between α and effective population size for 44 animal species. Additional evidence that there is more positive selection in larger populations stems from recent analyses of linked selection. Corbett-Detig et al. (2015) found increased evidence for linked selection in species with larger population sizes, though the mechanism driving this pattern is not immediately clear. Further, Nam et al. (2017) have suggested that across primates, species with larger population sizes have had more selective sweeps.

While this evidence suggests that adaptation could be mutation limited and that this could be driving the variation in α across species, it is important to note that other factors could be influencing the α statistic (Rousselle et al. 2018; Messer and Petrov 2013). As the denominator of α is the total number of observed differences between species, it is sensitive to the fixation of weakly deleterious mutations. For two populations with the same number of beneficial substitutions, the one with a higher number of substitutions due to weakly deleterious mutations will have a lower α. Indeed, because the number of fixed weakly deleterious mutations is

inversely related to population size (Ohta 1973, 1992), this effect could drive the correlation between α and population size. In support of this prediction, Galtier (2016) found that the rate of adaptive divergence (omega-a), which does not depend on the total number of divergent sites between species (Gossmann et al. 2012), showed no correlation with population size. Similar arguments have been made by Phifer-Rixey et al. (2012). Further, for humans, it has been suggested that α had been underestimated due to the presence of weakly beneficial mutations still segregating as polymorphisms (Galtier 2016; Uricchio et al. 2019). Indeed, methods that account for weakly beneficial mutations still segregating as polymorphisms infer slightly higher values of α = 0.24 between humans and chimpanzee, and α = 0.135 in the human lineage (Galtier 2016; Uricchio et al. 2019). In addition, population sizes of the outgroup and ancestral population determine the rate of fixation of weakly deleterious mutations in the outgroup lineage and in the ancestral population, and could potentially influence the estimate of α (Rousselle et al. 2018; McDonald and Kreitman 1991; Eyre-Walker 2002).

Other studies quantified positive selection by focusing on the proportion of beneficial mutations (p^+) and their selection coefficients (s^+). Boyko *et al.* (2008) found that by assuming a fraction (0 to 1.86%) of new mutations is positively selected, they could better match the frequency spectrum of polymorphisms and the counts of human-chimpanzee divergence. Models with weaker selection coefficients for beneficial mutations tended to have a higher proportion of positively selected mutations than models with stronger selection (Boyko et al. 2008). Several studies also have estimated p^+ and s^+ in *Drosophila* species and mice (Sella et al. 2009; Schneider et al. 2011; Elyashiv et al. 2016; Campos et al. 2017; Keightley et al. 2016; Booker and Keightley 2018). However, there has not been a systematic comparison across species.

110 Here we compare the amount of adaptive evolution in primates, rodents, and *Drosophila*.
111 We use two complementary approaches that quantify different aspects of the adaptive process.
112 First, we use improved modeling of weakly deleterious mutations and demographic models,
113 particularly correcting for the sizes of outgroup species and ancestral population to infer α.
114 Second, we estimate p^+ and s^+ of newly arising beneficial mutations by examining patterns of
115 polymorphism and divergence. We develop a composite likelihood framework to test whether
116 these parameters differ across taxa. This approach enables a more direct comparison of the
117 amount of beneficial mutations across species and is less confounded by the fixation of weakly
118 deleterious mutations.
119

120 **RESULTS**

121 ***Estimates of α for multiple species using the MK method***

122 We first estimated α from coding regions of primates, rodents, and *Drosophila*. We
123 analyzed published genomic datasets to obtain counts of synonymous and nonsynonymous
124 polymorphisms (P_S and P_N) and divergent sties between species (D_S and D_N). For computation of
125 α in humans, we used chimpanzee and macaque as outgroup species. For mice and *D.*
126 *melanogaster*, we used rat and *D. simulans* as the outgroup species, respectively. In total, 19.1
127 Mb of coding sequence for primates, 26.6 Mb of coding sequence for rodents, and 15.8 Mb of
128 coding sequence for *Drosophila* were used in our analysis (see Methods).

129 An extension of the McDonald-Kreitman test was used to estimate α (Smith and Eyre-
130 Walker 2002; Table 1; Supplemental Table S1). To examine the effect of slightly deleterious
131 mutations on α, we filtered the data with several minor allele frequency (MAF) cutoffs (Messer
132 and Petrov 2013; Fay et al. 2001; Charlesworth and Eyre-Walker 2008) (Supplemental Table

133 S2). For example, after removing low frequency polymorphisms with MAF less than 20% , the
134 estimated α is close to zero for the human-chimpanzee comparison (Table 1), consistent with
135 previous estimates (Boyko et al. 2008; Eyre-Walker and Keightley 2009). However, for the
136 human-macaque comparison, α is -0.22 (Table 1), suggesting that the choice of outgroup species
137 could greatly influence α. Nevertheless, these results suggest at most only a very small
138 proportion of nonsynonymous substitutions have been fixed by positive selection in primates. In
139 contrast, for the *D. melanogaster-D. simulans* and mouse-rat comparisons, the estimated α is
140 49% and 40%, respectively, with MAF filter at 20% (Table 1). Both of these estimates are
141 comparable to previous studies (Andolfatto 2005; Eyre-Walker and Keightley 2009; Phifer-
142 Rixey et al. 2012). These results suggest that the proportion of substitutions fixed by positive
143 selection varies drastically across species, and for taxa with larger population sizes, like rodents
144 and *Drosophila*, adaptive forces may have had a greater contribution to divergence.
145
146 ***Model-based inference of α***
147 Model-based approaches estimate α by contrasting the observed number of
148 nonsynonymous differences between species D_{NO} with the number expected under a
149 demographic model and a distribution of fitness effects (DFE) including only neutral and
150 deleterious mutations D_{NE} (Boyko et al. 2008; Eyre-Walker and Keightley 2009). The excess of
151 observed D_{NO} compared to the predicted D_{NE} is attributed to fixations driven by positive
152 selection. These methods also assume that the population sizes of outgroup species and the
153 ancestral population of the ingroup and outgroup are the same as the ancestral size of the ingroup
154 population (*Nanc.in*). We refer to this demographic model as the Simple model (Fig. 1A).

155 Using the Simple model, we first estimated the divergence time that best fit our data
156 using the observed D_S. We then predicted D_{NE} using this estimated divergence time, the gamma-
157 distributed DFE inferred in Huber et al. (2017), and the demographic model of the ingroup
158 species (Supplemental Text; Supplemental Table S3 and S4). We then estimated that α=11% for
159 humans and chimpanzee. This estimate is comparable to the inference by Boyko *et al.*, where
160 authors implemented a similar approach and estimated that approximately 10% of human-
161 chimpanzee nonsynonymous substitutions were fixed by positive selection (Boyko et al. 2008).
162 When using macaque as the outgroup species, we estimate that α is negative (Table 1). While it
163 is possible that this difference could reflect distinct evolutionary events experienced by different
164 outgroups, it could also be an artifact of the modeling assumptions. Previous estimates of the
165 human-chimpanzee ancestral population size (*Nanc*) range from 12,000 to 125,000 using
166 different datasets and methods (Chen and Li 2001; Hobolth et al. 2007; Burgess and Yang 2008;
167 Prado-Martinez et al. 2013; Schrago 2014). The estimated chimpanzee population size (*Nout)* is
168 around 30,000 (Prado-Martinez et al. 2013; Hvilsom et al. 2012; Fischer et al. 2004)
169 (Supplemental Table S5). However, the ancestral size inferred for the human lineage using
170 human polymorphism data is 7067, which is much smaller than all previous estimates of *Nanc*
171 and *Nout*. Using values of *Nanc* and *Nout* that are too small likely biases estimates of α because
172 more of the nonsynonymous substitutions are incorrectly attributed to the fixation of weakly
173 deleterious mutations, causing α to be under-estimated.
174 To more accurately model the larger *Nanc* and *Nout*, we use the Complex model which
175 allows *Nout* and *Nanc* to differ from *Nanc.in* (Fig. 1A). For humans, the larger *Nanc* is very
176 ancient, thus it does not affect the polymorphism pattern within humans (confirmed by
177 coalescent simulations, see Supplemental Text). We calculated the number of substitutions fixed

178 in the ingroup, outgroup, and ancestral populations. The total expected number of differences
179 between a pair of species is the sum of differences at all three stages. We first explored how *Nout*
180 and *Nanc* affect the inferred α. For the human-chimpanzee comparison, the inferred α changes
181 dramatically with different values of *Nout* and *Nanc*. Larger values result in larger estimates of α
182 (Fig. 1B). For example, when *Nout* = 30,000 (Prado-Martinez et al. 2013; Hvilsom et al. 2012;
183 Fischer et al. 2004) and *Nanc* = 60,000 (Chen and Li 2001; Hobolth et al. 2007; Prado-Martinez
184 et al. 2013), supported by many previous studies (Supplemental Table S5), α is approximately
185 24.6%. When using other values of *Nout* and *Nanc* within the ranges of previous estimates, the
186 corresponding estimates of α may differ, but remain above 20% (Fig. 1B). We next revisited the
187 human-macaque comparison under the Complex model (Supplemental Fig. S1), using *Nout* =
188 73,000 (Hernandez et al. 2007; Xue et al. 2016), *Nanc* = 48,000 (McVicker et al. 2009), and
189 changing the ingroup population size to 60,000 at human-chimpanzee divergence time to match
190 what we modeled in human-chimpanzee (Supplemental Table S4). Here we infer approximately
191 26.0% of human-macaque nonsynonymous substitutions were fixed by positive selection which
192 is comparable to what we found for the human-chimpanzee analysis. These estimates of α for
193 primates using the more realistic Complex demographic model are much higher than previous
194 estimates, implying that there is a greater contribution of positive selection to nonsynonymous
195 divergence than previously appreciated.

196 Similarly, we estimated α for *Drosophila* and rodents using the Complex demographic
197 model. For *Drosophila ,* it had been inferred that *D. simulans* have slightly larger N_e than *D.*
198 *melanogaster* (Andolfatto et al. 2011), so we set *Nout* to be 1.5× the current population size of *D.*
199 *melanogaster* (*Ncur*) at the species' split (Supplemental Table S4). For mice, a previous study
200 estimated that the outgroup rat species has an effective population size about fivefold lower than

201 wild house mice (Ness et al. 2012). Thus, we set the *Nout* to be 0.2× *Ncur* of mice (Supplemental
202 Table S4). Since there is limited knowledge of the population sizes of the ancestor of *D.*
203 *melanogaster* and *D. simulans*, and ancestor of mice and rat, for these two comparisons, we
204 assume *Nanc = Nout.* Using these Complex models for *D. melanogaster-D.simulans* and mouse-
205 rat, we estimated their α to be 60% and 41%, compared with 53% and 45% using the Simple
206 model, respectively (Table 1). The differences between these estimates reflect the importance of
207 accurately modeling the population size of outgroup species for calculations of α.
208 We estimated α for substitutions that occurred exclusively on the human lineage, using
209 the human-macaque alignment to polarize sequence differences between human and chimpanzee.
210 We estimate that α = 6.2% using the Simple model, and 16.0% using the Complex model (Table
211 1).
212 To compare our estimates of α to those from another model-based method that assumes
213 *Nanc=Nout=Nanc.in*, we used *DFE-alpha*, to infer α for our three species pairs. Using this
214 method, α is estimated to be 24% and 2% for humans using chimpanzee and macaque as
215 outgroup respectively, 71% for *D. melanogaster-D. simulans*, and 51% for mouse-rat (Table 1).
216 These estimates are all higher compared to estimates from Simple models. However, the
217 estimates of α for primates differ significantly depending on whether the macaque or chimpanzee
218 is used as the outgroup for humans.
219
220 ***Testing whether p^+ and s^+ differ across species***
221 We next estimated the DFE including new beneficial mutations. Our model of the DFE
222 includes two additional parameters compared to the base model that only includes deleterious
223 mutations. For each species, we estimate the proportion of new mutations that are beneficial (p^+)

224 and their selection coefficient (s^+). We then test whether these two parameters differ across
225 species.

226 The number of nonsynonymous differences between a pair of species (D_N) is assumed to
227 be Poisson-distributed (Sawyer and Hartl 1992), with rate parameter equal to:

228 $$E[D_N] = 2N\mu[\int G(s)u(s)\,(1-p^+) + u(s^+)p^+] \qquad \text{eq.(1)}$$

229 where $G(s)$ is the DFE of deleterious and neutral mutations from Huber et al. (2017), $u(s)$ is the
230 fixation probability (Kimura 1962) of deleterious and neutral mutations, $u(s^+)$ is the fixation
231 probability of beneficial mutations, and p^+ is the proportion of new mutations that are beneficial.
232 We then use a Poisson log-likelihood function for D_N in each species and a series of likelihood
233 ratio tests (LRTs) to determine whether p^+ and s^+ differ across primates, rodents, and *Drosophila*
234 (see Methods).

235 Using this framework, we find that the full model H1, where each taxon is allowed to
236 have its own p^+ and s^+, fits D_N significantly better than the constrained null model, where p^+ and
237 s^+ are constrained to be the same across all three taxa (LRT statistic Λ=124,974, df=4, $P<10^{-16}$;
238 Fig. 2; Supplemental Fig. S2; Supplemental Table S6).

239 We estimate that humans have a higher proportion of beneficial nonsynonymous
240 mutations than *D. melanogaster* and mice (Supplemental Table S6 and Fig. 2). Specifically, we
241 estimate that approximately 1.55% of new nonsynonymous mutations in humans are beneficial
242 with s^+ of approximately 1.12×10^{-4} (outgroup: chimpanzee), approximately 0.0675% of new
243 nonsynonymous mutations in *D. melanogaster* are beneficial with s^+ of approximately 1.58×10^{-5},
244 and approximately 1.02% of new nonsynonymous mutations in mice are beneficial with s^+ of
245 1.60×10^{-5} (Supplemental Table S6). Models with a larger s^+ tend to have a lower proportion of
246 positively selected mutations than models with smaller s^+. Consequently, the likelihoods of these

247 parameter values can be very close to the likelihoods at the MLEs. We also compared p^+ and s^+
248 between pairs of taxa (*i.e.* primate *vs.* rodent; primate *vs. Drosophila*; rodent *vs. Drosophila*). In
249 all pairwise tests (regardless of outgroup or demography), the model where each species has its
250 own p^+ and s^+ fits the observed D_N significantly better than a model where p^+ and s^+ are
251 constrained to be the same in the tested two taxa (Supplemental Table S6).

252 We next investigated whether it is possible that either p^+ or s^+ is the same across taxa but
253 the other parameter varies. Specifically, we allowed p^+ to differ across primates, rodents, and
254 *Drosophila*, then explored whether a model with the same s^+ could fit all species. This is shown
255 in conditional likelihood plots, where assuming the same s^+ for all species, humans would need a
256 higher proportion of beneficial mutations compared to mice and *D. melanogaster* to match the
257 observed D_N (Fig. 3A). Similarly, allowing s^+ to differ across species, a model with the same p^+
258 across all species could fit the data. When we forced the same p^+ for all species, s^+ for beneficial
259 mutations in humans would be larger compared to that in mice and *D. melanogaster* (Fig. 3B).
260 However, for the same p^+ value, s^+ could not be the same in all species. Similarly, for the same
261 s^+ value, p^+ could not be the same across species.

262 Motivated by the observation that larger values of p^+ and smaller values of s^+ can fit the
263 data as well as models with smaller values of p^+ and larger values of s^+, we also estimated a
264 composite parameter p^+s^+, the product of p^+ and s^+. We find clear evidence that regardless of the
265 model of ancestral demography or outgroup, humans have a significantly higher p^+s^+ than do *D.*
266 *melanogaster* and mice (Fig. 4). This can be seen by looking at the log-likelihood curves, which
267 are quite peaked, with little overlap across species. Thus, approximate 95% confidence intervals
268 on p^+s^+ for the different species do not overlap, implying more positive selection in humans than
269 in *D. melanogaster* and mice.

270

271 ***Testing whether γ+ and p+ differ across species***

272 Humans, *D. melanogaster*, and mice have drastically different population sizes, which
273 can influence the efficacy of selection within each species. Thus, we next examined whether the
274 selection coefficient scaled by current population size ($\gamma^+=2Ns^+$) and p^+ differ across primates,
275 rodents, and *Drosophila*.

276 We find the model (Full model H1) where each taxon has its own different γ^+ and p^+ fits
277 the observed D_N significantly better than a model (constrained model H0) where γ^+ and p^+ are
278 constrained to be the same across all three taxa (LRT statistic Λ=3,541; df=4, $P<10^{-16}$, Fig. 5;
279 Supplemental Fig. S2; Supplemental Table S6).

280 Under the full model, we estimate that approximately 1% of new nonsynonymous
281 mutations in humans are beneficial with γ^+ of 6.05, approximately 2% of new nonsynonymous
282 mutations in *D. melanogaster* are beneficial with γ^+ of 4.92, and approximately 4% of new
283 nonsynonymous mutations in mice are beneficial with γ^+ of 3.76 (Supplemental Table S6).
284 Models with larger γ^+ tended to have a lower proportion of positively selected mutations than
285 models with smaller γ^+, and the likelihoods can be very close to those at the MLEs. The current
286 population sizes are 16,539, 7,616,700, 488,948 for humans, *D. melanogaster* and mice,
287 respectively. As a result, we are searching for p^+ within the same range of γ^+ (see Methods), but
288 markedly different ranges of s^+ for these three species. Thus, the relative ordering of the MLEs
289 of p^+ across species considering γ^+ is not necessarily the same as that for the s^+ results described
290 above.

291 We also compared γ^+ and p^+ between pairs of taxa. We find that for the human- *D.*
292 *melanogaster* and human-mice pairs, the models where each species has its own different γ^+ and

293 p^+ fit the observed D_N significantly better than a model where $\boldsymbol{\gamma}^+$ and p^+ are constrained to be the
294 same in the tested two taxa (Supplemental Table S6). This result is robust regardless of outgroup
295 species. However, we cannot reject the hypothesis that mice and *D. melanogaster* have same $\boldsymbol{\gamma}^+$
296 and p^+ (Supplemental Table S6).

297 We next investigated whether it is possible that either $\boldsymbol{\gamma}^+$ or p^+ is the same across taxa,
298 while the other parameter varies. With the same $\boldsymbol{\gamma}^+$ for all species, humans would need a lower
299 proportion of beneficial mutations compared to mice and *D. melanogaster* to fit the observed D_N
300 (Supplemental Fig. S3A). When we constrain p^+ to be the same for all taxa, humans have a
301 smaller $\boldsymbol{\gamma}^+$ for beneficial mutations (Supplemental Fig. S3B). However, for the same p^+ value, $\boldsymbol{\gamma}^+$
302 cannot be the same in all taxa. Similarly, for the same $\boldsymbol{\gamma}^+$ value, p^+ cannot be the same across
303 taxa. We also estimated a composite parameter $p^+\boldsymbol{\gamma}^+$, the product of p^+ and $\boldsymbol{\gamma}^+$. We find that $p^+\boldsymbol{\gamma}$
304 $^+$ is not as distinct across different taxa as is p^+s^+. In the Complex models, humans have a
305 smaller $p^+\boldsymbol{\gamma}^+$ than mice. However, the log-likelihood curves of $p^+\boldsymbol{\gamma}^+$ overlap between *D.*
306 *melanogaster* and mice, and between *D. melanogaster* and humans, suggesting they are not
307 significantly different (Supplemental Fig. S4).

308

309 ***Effects of biased gene conversion and hypermutable*** CpG ***sites***

310 Biased gene conversion (BGC) is the preferred transmission of G/C alleles (S: strong
311 alleles) at the expense of A/T alleles (W: weak alleles). This process is common in mammals and
312 could impact patterns of genetic diversity (Duret and Galtier 2009; Lachance and Tishkoff 2014;
313 Bolívar et al. 2015) and bias estimates of rate of positive selection (Corcoran et al. 2017),
314 especially when comparing between taxa with BGC and taxa without BGC, *i.e. D. melanogaster*
315 (Robinson et al. 2014). Further, methylated CpG sites in mammals have a higher mutation rate to

316 T alleles due to deamination of the C nucleotide (Sved and Bird 1990; Duncan and Miller 1980),
317 which could possibly bias inferences of selection.

318 To test whether BGC and hypermutable CpG sites drive the observed pattern of positive
319 selection across primates, rodents, and *Drosophila*, we filtered primate and rodent data to keep
320 only strong to strong or weak to weak mutations (herein called SSWW mutations), which are not
321 affected by BGC and are not CpG changes (Supplemental Text, Supplemental Fig. S5). We then
322 re-inferred α. For primates, α is comparable to that without filtering (Table 1). For rodents,
323 however, α is substantially lower than that before filtering, suggesting that biased gene
324 conversion and CpG mutational processes may account for some of the nonsynonymous
325 differences between mouse and rat.

326 Removing the effect of BGC and CpG sites in primates and rodents, we again quantify
327 and compare the strength and proportion of new beneficial mutations across all three taxa. The
328 model where each taxon has its own p^+ and s^+ fits the observed D_N significantly better than a
329 model where p^+ and s^+ are constrained to be the same across all three taxa (LRT statistic Λ=825,
330 df=4, $P<10^{-16}$; Supplemental Fig. S6; Supplemental Table S6). Models comparing each pair of
331 taxa (*e.g.* primates *vs.* rodents; primates *vs. Drosophila*; rodents *vs. Drosophila*) suggest that
332 each taxon has its own unique p^+ and s^+, regardless of demography (Supplemental Table S6).
333 Allowing p^+ to differ across taxa, a model with the same s^+ across all taxa could fit the data, and
334 *vice versa.* When we force the same s^+ for all species, humans still have the highest proportion of
335 new beneficial mutations (Supplemental Fig. S6E). Constraining p^+ to be the same for all
336 species, humans have the largest selection coefficient (Supplemental Fig. S6F).

337 Similarly, the model where each taxon has its own p^+ and $\boldsymbol{\gamma}^+$ fits the observed D_N
338 significantly better than a model where p^+ and $\boldsymbol{\gamma}^+$ are constrained to be the same across all three

339 taxa (LRT Λ=4496, df=4, $P<10^{-16}$; Supplemental Table S6 and Fig. S7). Models comparing each
340 pair of taxa suggest that each taxon has its own unique p^+ and $\boldsymbol{\gamma}^+$, regardless of demography
341 (Supplemental Table S6). Allowing p^+ to differ across species, a model with the same $\boldsymbol{\gamma}^+$ across
342 all taxa could fit the data, and *vice versa*. When we constrain $\boldsymbol{\gamma}^+$ to be the same for all species, *D.*
343 *melanogaster* have the highest proportion of new mutations being beneficial, and mice have the
344 lowest proportion of new mutations that are beneficial. When we constrain p^+ to be the same for
345 all species, *D. melanogaster* have the largest $\boldsymbol{\gamma}^+$, and mice have the smallest $\boldsymbol{\gamma}^+$(Supplemental
346 Fig. S7).

347 Lastly, we estimated two composite parameters, p^+s^+ and $p^+\boldsymbol{\gamma}^+$ for SSWW mutations.
348 Humans again have a significantly higher p^+s^+ than *D. melanogaster* and mice (Supplemental
349 Fig. S8), suggesting more positive selection in humans than in *D. melanogaster* and mice.
350 Similar to the full dataset, $p^+\boldsymbol{\gamma}^+$ is not as distinct across different species as p^+s^+. Under the
351 Complex model, we find that humans and *D. melanogaster* have a significantly (*i.e.* the log-
352 likelihood curves do not overlap within 2 units of the MLEs) larger $p^+\boldsymbol{\gamma}^+$ than mice, and the log-
353 likelihood curves of $p^+\boldsymbol{\gamma}^+$ for humans and *D. melanogaster* overlap near the MLEs
354 (Supplemental Fig. S8).
355

356 **DISCUSSION**

357 We have quantified the amount of adaptive evolution in multiple species with differing
358 degrees of complexity and population size using two different approaches. First, we examined
359 the proportion of nonsynonymous substitutions fixed by positive selection and found that this
360 proportion is higher in *Drosophila* than in rodents and primates, consistent with prior work
361 (Andolfatto 2005; Eyre-Walker and Keightley 2009; Boyko et al. 2008; Fay 2011). However,

362 after correcting for the population sizes of the outgroup and ancestral population, we infer that α
363 is much higher in primates than what was inferred in previous studies. Second, we show that the
364 DFE of new beneficial mutations differs across species. The species with the smaller population
365 size and greater complexity (*i.e.* humans) has stronger and/or more abundant new beneficial
366 mutations than the other two species with much larger population sizes (*i.e.* mice and *D.*
367 *melanogaster*). These results are robust to the choice of outgroups, BGC, and hypermutable CpG
368 sites.

369 One major improvement of our method to infer α over previous similar approaches from
370 Boyko et al. and *DFE-alpha* (Boyko et al. 2008; Eyre-Walker and Keightley 2009) is that we
371 allow the outgroup and ancestral population sizes to differ from the ancestral population size of
372 the ingroup. In Boyko *et al.* (2008), the outgroup population size is assumed to be the same as
373 that found in the ancestral ingroup population. *DFE-alpha* allows for inference of demographic
374 parameters of one- to three- epoch models, and the outgroup population size is assumed to be the
375 same as the ancestral ingroup population. When considering species like humans in relation to
376 other primates, like chimpanzee or macaque, this assumption certainly does not hold as primate
377 species have population sizes at least several fold larger than the estimated ancestral human
378 population size of approximately 7,000 individuals (Chen and Li 2001; Hobolth et al. 2007;
379 Burgess and Yang 2008; Prado-Martinez et al. 2013; Schrago 2014; Hernandez et al. 2007;
380 McVicker et al. 2009; Hvilsom et al. 2012; Wall 2013; Xue et al. 2016). The sizes of the
381 outgroup and ancestral population matter because they affect the fixation probability of weakly
382 deleterious alleles (Kimura 1983; Ohta 1973, 1992). As such, the number of nonsynonymous
383 substitutions attributed to weakly deleterious mutations is highly affected by the population sizes
384 of the outgroup and ancestral population. Consequently, estimates of α are affected as well. Our

385 approach includes a more complex demographic model that allows the ancestral and outgroup
386 populations to have their own sizes (*Nanc* and *Nout*). By using these more realistic population
387 sizes, the α estimates we obtained for primates are similar when using chimpanzee or macaque as
388 outgroup species. This is strong evidence that our method is more accurate as all the other
389 methods give drastically different estimates of α using these two different outgroups.
390 Interestingly, Eyre-Walker and Keightley (2009) also suggested that α in humans could be as
391 high as 0.31 if the effective population size of humans and macaques was much higher than
392 10,000 until very recently, foreshadowing our current estimates. Future studies of adaptive
393 substitutions should carefully consider ancestral and outgroup population sizes and should use
394 statistical methods that model them realistically.

395 Here we have quantified adaptive evolution from two different perspectives. First, we
396 estimate the proportion of adaptive nonsynonymous substitutions between species, α. This
397 statistic measures the endpoint where a number of factors such as demography, genetic drift, and
398 natural selection all come into play. Second, we estimate the DFE of newly arising beneficial
399 mutations, *i.e.* p^+ and s^+. This approach aims to understand the properties of new beneficial
400 mutations, the beginning point where beneficial mutations appear and enter the population. Thus,
401 it is possible that these two approaches can yield qualitative opposite results. Indeed, we have
402 shown that *D. melanogaster* have the largest values of α, but the smallest p^+s^+.

403 We previously found 15% of nonsynonymous mutations in humans are weakly beneficial
404 (Huber et al. 2017). Importantly, because Huber *et al.* only analyzed polymorphism data, they
405 did not consider strongly beneficial mutations that became substitutions between species. Our
406 present study leverages genome sequences of several related species pairs to estimate the
407 proportion of strongly beneficial ($s^+>10^{-5}$) mutations that are fixed between species. Weakly

408 beneficial mutations are already accounted for in our model using the DFE from Huber *et al.*
409 (2017) as many weakly beneficial mutations are likely segregating as polymorphisms.
410 Intriguingly, we find that humans have a higher proportion of strongly beneficial mutations than
411 *D. melanogaster*, mirroring the qualitative trend seen for weakly beneficial mutations in Huber *et*
412 *al*. (2017). In the context of human evolution, it has been shown that weakly beneficial mutations
413 that are still segregating could result in an underestimate of α (Uricchio et al. 2019; Galtier
414 2016). Thus, the estimate of α in humans could be even higher if adaptive polymorphisms were
415 taken into account. Alternatively, our current approach of modeling the complex demography in
416 the outgroup and ancestral population should correct for some of the bias in inferring α due to
417 weakly beneficial mutations still segregating as polymorphisms. The reason for this is that
418 weakly beneficial mutations still segregating as polymorphisms will be accounted for in the
419 parametric DFE fit to the site frequency spectrum (SFS; as discussed above in the context of
420 Huber et al. 2017). A parametric DFE including only deleterious and neutral mutations will treat
421 this class of weakly beneficial mutations as nearly neutral (Tataru et al. 2017), inflating the
422 expected divergence that can be accounted for by non-adaptive forces. Modeling the complex
423 demography reduces the number of fixations from nearly neutral mutations that are treated in the
424 model to be non-adaptive, including those from segregating weakly beneficial mutations.
425 Our estimate of α for human lineage is 16.0% using the Complex model, which is
426 comparable to the estimate of human-lineage α by Uricchio *et al.* (2019), despite the use of
427 different analytical approaches. α is expected to be lower on the human lineage as compared to
428 the chimpanzee or macaque lineage due to the higher proportion of weakly deleterious amino
429 acid substitutions on the human lineage to their smaller population size (Ohta 1973, 1992). For
430 *D. melanogaster*, using the Complex model we estimate $p^{+}\boldsymbol{\gamma}^{+}$ to be ~0.1 which is within a factor

431 of 2 of a previous estimate of Keightley et al. (2016). For mice, using the Complex model, we
432 estimate $p^+\boldsymbol{\gamma}^+$ to be ~0.15 which is somewhat greater than the value of ~0.05 inferred in Booker
433 and Keightley (2018). The differences in estimates could be due to the use of different methods
434 and models, such as our detailed modeling of the ancestral and outgroup population sizes.
435
436 We make several key modeling assumptions. First, we assume that the DFE is the same
437 between the ingroup and outgroup for each pair of species (*e.g.* humans and chimpanzee have the
438 same DFE). This assumption could be relaxed by using only polymorphism data to infer the
439 beneficial DFE (Tataru et al. 2017), though not including divergence to an outgroup species
440 considerably reduces the power to infer positive selection (Booker 2019). Second, our inference
441 of p^+ and s^+, as well as related approaches (Schneider et al. 2011; Tataru et al. 2017; Booker and
442 Keightley 2018), make the assumption of selection starting from a single mutation, since we use
443 the fixation probability of a mutation introduced as a single copy. Selection on standing variation
444 (*i.e.* one type of soft sweep) might bias the parameter estimates, though the meaning of p^+ and s^+
445 are not as clear under models with soft sweeps. α, however, should be accurately estimated even
446 as long as the beneficial mutation reaches fixation. Furthermore, as our approach only focuses on
447 strongly beneficial mutations that contribute to divergence, it is not sensitive to types of selection
448 that do not reach fixation. These include another type of soft sweeps (Pritchard et al. 2010),
449 where multiple independent beneficial mutations in the same gene are selected simultaneously,
450 but no mutation becomes fixed, as well as polygenic adaptation where beneficial alleles only
451 slightly increase in frequency, without reaching fixation. A last limitation comes from the model
452 itself. It has been suggested that models where s^+ does not change over time may not model the
453 complexity of adaptive walks, where the first beneficial mutation may have a more strongly

454 beneficial effect on fitness than subsequent beneficial mutations (Gillespie 2004; Lourenço et al.
455 2013). Thus, our estimates of p^+ and s^+ should be interpreted in this context as the average values
456 over longer time periods and over different genetic backgrounds, rather than literal values that
457 have stayed constant over time. In fact, our findings show that p^+ and s^+ have changed over deep
458 evolutionary time, pointing to their dynamic nature.

459 One previous explanation for varying estimates of α across species was that adaptation is
460 mutation limited and there are more beneficial mutations in organisms with larger population
461 sizes. This view was not supported by conceptual arguments by Gillespie (2004) who suggested
462 that the rate of environment change will matter more than the population size in determining the
463 rate of adaptive evolution. The simulation study by Lourenço et al. (2013) that considered a
464 changing DFE over time in the context of Fisher's geometric model found that the population
465 size only weakly related to α. Instead, the rate at which the environment changed was an
466 important predictor of the amount of adaptive evolution, as environmental shifts moved the
467 population from the fitness optimum, creating the opportunity for new beneficial mutations.
468 Further, Rousselle et al. (2019) recently found a weak negative correlation between the amount
469 of adaptive evolution and the amount of genetic diversity in modern populations, which supports
470 the models of Lourenco *et al.*(2013) and Gillespie (2004). However, not all studies are in
471 agreement on the role of the environment as Connallon and Clark (2015) found that
472 environmental heterogeneity reduces the fraction of beneficial mutations by inflating the
473 standardized mutation size in Fisher's geometric model. Lourenço et al. (2013) also found that
474 organismal complexity, here defined as the number of phenotypes under selection, was a key
475 predictor of the amount of adaptive evolution within species. Through a "cost of complexity",
476 more complex organisms have a harder time adapting to new environmental conditions due to

477 the additional constraints imposed by the increased number of traits under selection. As such,
478 adaptive walks require more beneficial mutations (Orr 1998).
479 Our results presented here are in broad agreement with the conceptual model of Lourenço
480 et al. (2013). Specifically, we do not find that species with larger population sizes (*i.e. D.*
481 *melanogaster*) have more beneficial mutations. Instead, we find that p^+ (as well as p^+s^+) is
482 higher in humans than in *D. melanogaster* or mice. Second, while it is hard to precisely define
483 organismal complexity, previous work has found more protein-protein interactions in humans
484 than in *Drosophila* (Valentine et al. 1994; Stumpf et al. 2008), suggesting that humans may be
485 more complex than *Drosophila*. If this is the case, then our findings of a higher p^+ (and p^+s^+) in
486 humans than *D. melanogaster* and mice supports the arguments from Lourenço et al. (2013) that
487 adaptive walks after an environmental shift are less efficient and require more steps (*i.e.*
488 beneficial mutations) in more complex organisms, leading to higher p^+ in complex organisms.
489 Additionally, differences in the degree of environmental change across species could also
490 contribute to the disparate inferences of p^+s^+ across taxa. While it is hard to say which species
491 has experienced more environmental shifts, it has been suggested that those species with longer
492 generation times, like primates, may experience more environmental change per generation than
493 species with shorter generation times, like *Drosophila* or rodents (Rousselle et al. 2019;
494 Romiguier et al. 2014). Our finding of higher p^+ in humans than *Drosophila* supports this
495 intriguing prediction.
496
497 **METHODS**
498 ***Polymorphism and divergence data for humans, mice, and D. melanogaster***

499 For humans, we used polymorphism data from 112 individuals from Yoruba in Ibadan,
500 Nigeria (YRI) from the 1000 Genomes Project (1000 Genomes Project Consortium 2012).
501 Published genome alignments of human and chimpanzee (hg19/pantro4), and human and
502 *Macaca mulatta* (hg19/rheMac3) were downloaded from the UCSC genome browser
503 (http://hgdownload.soe.ucsc.edu/goldenPath/hg19/). For *D. melanogaster*, we used the
504 Drosophila Population Genomics Project phase 3 data, including 197 African *D. melanogaster*
505 lines from Zambia, Africa (Lack et al. 2015). For divergence, *D. melanogaster* and *D. simulans*
506 genic alignments (Dmel v5/Dsim v2) were extracted from the multi-species alignments from Hu
507 et al. (2013). Only autosomal regions were used in our analysis. Human and *D. melanogaster*
508 polymorphism data were filtered and down-sampled to 100 chromosomes as described in Huber
509 et al. (2017).
510 For mice, raw data (fastq) was downloaded for 10 *M. m. castaneus* individuals that were
511 collected in the northwest Indian state of Himachal Pradesh (Halligan et al. 2010, 2013). Reads
512 were mapped against mouse genome mm9 using bwa (Li and Durbin 2009) and stampy (Lunter
513 and Goodson 2011). Duplicate reads were marked using Picard, and further pre-processing was
514 done following GATK Best Practice guidelines (McKenna et al. 2010). Variants were called
515 using the GATK UnifiedGenotyper and filtered using the GATK VQSR using Affymetrix Mouse
516 Diversity Genotyping Array sites (Yang et al. 2009). We further filtered the dataset to only retain
517 sites with a sample size of at least 16 chromosomes and down-sampled all sites with larger
518 sample size to a sample size of 16 chromosomes using the hypergeometric probability
519 distribution. Published genome alignments of mice and rat (mm9/rn5) were downloaded from
520 UCSC (http://hgdownload.soe.ucsc.edu/goldenPath/mm9/vsRn5/axtNet/). For each species,

521 polymorphism and divergence data were intersected, and only coding regions shared by both
522 datasets were used in our analysis.
523 In total, 19.1Mb of coding sequences for primates, 26.6 Mb of coding sequences for
524 rodents and 15.8Mb of coding sequences for *Drosophila* were included. The nonsynonymous
525 and synonymous total sequence lengths (L_{NS}, L_S) were estimated using multipliers of $L_{NS} = 2.85$
526 $\times L_S$ in *D. melanogaster*, and $L_{NS} = 2.31 \times L_S$ in mammals from Huber et al. (2017). In these
527 filtered coding sequences, we annotated synonymous and nonsynonymous sites in both
528 polymorphism and substitution data for each species. Human variants were annotated using the
529 SeattleSeq Annotation pipeline (http://snp.gs.washington.edu/SeattleSeqAnnotation138/). Mice
530 and Drosophila variants were annotated using SnpEeff v3.6 using the mice NCBIM37.66
531 annotation database and the *D. melanogaster* BDGP5.75 annotation database, respectively. Sites
532 that are annotated as near-splice, or loss of function were removed. The ratio of
533 nonsynonymous/synonymous differences between human and chimp sequences in our dataset is
534 approximately 0.65, which is consistent with several previous reports from different datasets
535 (Bustamante et al. 2005; Torgerson et al. 2009; Enard et al. 2014).
536 From the down-sampled polymorphism data, we calculated the synonymous and
537 nonsynonymous SFS, and used the folded SFS for all further inferences to avoid
538 misidentification of the ancestral state.
539
540 ***Model-based estimates of α***
541 To implement a model-based approach to estimate α, for each pair of species, we need a
542 demographic model and a DFE for neutral and deleterious mutations to predict the D_{NE} that is
543 accounted for by neutral and deleterious mutations. For primates and *Drosophila*, we use

544 demographic and DFE parameters from Huber *et al.* (2017; Supplemental Table S3). For rodents,
545 we conducted our own inference of these parameters by summarizing the polymorphism data in
546 mice by the folded SFS (Supplemental Text).

547 To compute the expected divergence between species, we computed the divergence
548 accumulated in ingroup population, outgroup population and ancestral population separately and
549 summed them up. The divergence in the ingroup and outgroup population is a function of
550 divergence time, effective population size, mutation rate, and selection coefficient and was
551 calculated according to equation 13 in Sawyer and Hartl (1992). We computed the expected
552 divergence under a gamma DFE model by Monte Carlo integration using one million gamma
553 distributed selection coefficients. The contribution of the ancestral population to divergence
554 between two species was computed numerically based on the diffusion equation, using *prfreq*
555 (Boyko et al. 2008) and assuming the same gamma DFE. These calculations are implemented in
556 our program *predicDiv* (https://github.com/LohmuellerLab/predicDiv). For both the Simple and
557 the Complex models, we first estimate the divergence times (Supplemental Table S4) that fit the
558 observed number of synonymous differences between a pair of species because there is a wide
559 range of divergence times from the literature for each species. Here the number of synonymous
560 differences equals 2 × divergence time × mutation rate. Second, using this divergence time,
561 demography, and DFE inferred from Huber *et al.*(2017), or as described above for mice, we
562 estimated the expected number nonsynonymous differences (D_{NE}) according to Sawyer and Hartl
563 eqn 13 (Sawyer and Hartl 1992; Boyko et al. 2008). Then, α is calculated as

564 $$\alpha = \frac{D_{NO} - D_{NE}}{D_{NO}} \quad , \qquad \text{eq. (2)}$$

565 where D_{NO} is the observed number of nonsynonymous differences between species.

566

567 ***DFE-alpha***

568 Data files and the program v2.15 were downloaded from the following link:
569 http://www.homepages.ed.ac.uk/pkeightl//dfe_alpha/download-dfe-alpha.html. Folded
570 synonymous and nonsynonymous SFS were used as input in the inferences. The
571 *est_alpha_omega* program was used to estimate the proportion of adaptive divergence.

572

573 ***Composite likelihood approach for testing whether p^+ and s^+ differ across species***

574 We first used *predicDiv* and *prfreq* to generate a look-up table for the expected number
575 of nonsynonymous differences between species for a range of s^+ (10^{-5}-10^{-2}) for each species. We
576 focused on this range to capture strongly advantageous mutations. Given a demographic model,
577 we again assume a substitution rate according to equation 13 in Sawyer and Hartl (1992). The
578 contribution of the ancestral population to the divergence between two species is computed by
579 numerically solving the diffusion equation using *predicDiv* and *prfreq* (Boyko et al. 2008). For
580 each species, we then did a grid search of $\log_{10}(s^+)$ (-5 to -2) and p^+(0-7.5%). We are interested
581 in this range of strong s^+ because weakly beneficial mutations still segregating as polymorphisms
582 and are accounted for by the DFE fit to the SFS. We use a Poisson log-likelihood function to
583 calculate the log-likelihood (LL) for each combination of s^+ and p^+. We find the MLE of s^+ and
584 p^+ for each taxon under each demographic model that maximizes the LL and best fit the observed
585 D_N. This is the full model (H1) where each taxon (*i.e.* primates, rodent and *Drosophila*) is
586 allowed to have its own s^+ and p^+. Our H0 hypothesis is the constrained model, where two or
587 three taxa have the same s^+ and p^+. The LL of the constrained model is the sum of LL for each s^+
588 and p^+ for each taxon under comparison. We then found the MLE for the constrained model and
589 calculate the likelihood ratio between H1 and H0.

590

591 ***Composite likelihood approach for testing whether p^+ and γ^+ differ across species***

592 Similarly, we used *predicDiv* and *prfreq* (Boyko et al. 2008) to generate a look-up table
593 for the expected number of nonsynonymous differences for a range of γ^+ (1-10^3) for each taxon
594 under each demographic model. For each species, we performed a grid search of $\log_{10}(\gamma^+)$ (0-3)
595 and p^+(0-7.5%). Note, because effective population sizes differ over several orders of magnitude
596 across our three taxa, we are searching across drastically different ranges of s^+ as compared to
597 our previous inference described above. We again use a Poisson log-likelihood function to
598 calculate the LL for each combination of γ^+ and p^+ and use a similar LRT framework as
599 described above for s^+ and p^+.

600

601 ***Composite parameters p^+s^+ and $p^+\gamma^+$***

602 We examined two composite parameters, the product of p^+ and s^+ and the product of p^+
603 and γ^+ for each taxon. Multiple combinations of parameters could give the same product p^+s^+
604 and $p^+\gamma^+$and distinct combinations could have different LL. Thus we found the values of p^+ and
605 s^+ that gave the highest LL for each p^+s^+ value (and similarly each p^+ and $\gamma^+$for each $p^+\gamma^+$).
606 Values of $\log_{10}(p^+s^+)$ and $p^+\gamma^+$were rounded to three digits prior to this comparison.

607

608 ***Conditional log-likelihoods***

609 To examine whether primates, rodents, and *Drosophila* could have the same s^+ or p^+, we
610 examined the conditional log-likelihoods. To make the conditional log-likelihood curve for p^+,
611 for each s^+ value, we find the p^+ that maximizes the LL as well as the p^+ values that have a LL
612 within three LL units of this maximum LL for this s^+ (*i.e.* $p^+| s^+$). To make the conditional log-

613 likelihood curve for s^+, for each p^+ value, we look for the s^+ that maximizes the log-likelihood as
614 well as the s^+ values that have a LL within three LL units of this maximum LL for this p^+ (*i.e.* $s^+|$
615 p^+). The same approach was used to construct the conditional log-likelihood curve for p^+ and $\boldsymbol{\gamma}^+$.
616

617 ***Estimating α on the human lineage***

618 Human-chimpanzee differences were polarized by the macaque sequence. Differences
619 between human and chimpanzee were assigned to human lineage if the bases differ between
620 human and macaque, but were the same between chimpanzee and macaque in the pairwise
621 genome alignments. Differences that are in regions where the human and macaque sequences
622 were un-alignable and sites that differ among human, chimp, and macaque cannot be polarized
623 (3.8% total) and were filtered out. The total length of coding regions was scaled by this filter
624 accordingly. A total of 30,530 synonymous substitutions and 20,013 nonsynonymous differences
625 were observed on human lineage. We assume the human lineage and the outgroup lineage
626 contribute equally to neutral D_S, thus the total D_S between human and chimpanzee would be
627 61,060. We then adjusted divergence time to match predicted D_S to 61,060, and use this adjusted
628 divergence time, DFE of deleterious mutations and demography of human to predict D_N as
629 described in *Model-based estimates of α*. The human lineage α is then calculated using equation
630 (2).
631

632 ***Filtering to only include sites not affected by biased gene conversion or CpG hypermutation***

633 Full polymorphism and substitutions datasets of primates and rodents were filtered to
634 keep only strong to strong or weak to weak (SSWW) mutations because these changes were not
635 affected by BGC or increased mutation rates due to deamination of methylated CpG sites. These

636 changes include only A to T, T to A, C to G and G to C changes. These changes are only a small
637 subset of all variable sites. The nonsynonymous and synonymous sequence lengths (L_{NS}, L_S)
638 depend on the transition/transversion ratio and the CpG mutational bias. SSWW mutations are all
639 transversions and do not included any CpG mutations, leading to a multiplier of L_{NS} = 5.21 x L_S
640 in both primates and rodents. To compute this: 1) we used numbers of 0-, 2-, 3- and 4- fold sites
641 in the human exome from Veeramah et al. (2014); 2) we consider all 2-fold sites to be
642 nonsynonymous (because SSWW mutations are all transversions); and 3) we do not consider a
643 mutational bias of CpG sites (because CpG sites are not included in the SSWW set). In addition,
644 because SSWW mutations are only a small subset of all mutations, mutation rates need to be
645 scaled down to the SSWW specific mutation rate. To estimate the demographic parameters and
646 DFE for SSWW polymorphisms in rodents, first, we used the observed number of synonymous
647 SSWW polymorphisms to estimate the mutation rate for mice SSWW mutations to be $5.99\times10^{-}$
648 ^{10}. Then, using the SFS for SSWW synonymous polymorphisms, we inferred that the ancestral
649 population size in mice is approximately 246,256 which expanded 1.7-fold approximately
650 262,000 generations ago (Supplemental Table S3). Conditional on this demographic model, we
651 estimated the DFE for new nonsynonymous SSWW mutations in mice. We assume that the DFE
652 follows a gamma distribution and estimate its shape parameter α to be 0.21 and scale parameter
653 beta to be 0.050 (Supplemental Table S3). These estimates are within the same magnitude of the
654 estimates from the full dataset and a previous study (Huber et al. 2017). We re-estimated the
655 mouse-rat divergence time that fits best with the observed SSWW D_S. We then re-inferred p^+, s^+,
656 and $\boldsymbol{\gamma}^+$ as done previously, using the filtered data, new mutation rates, and new values of L_{NS}.
657
658

ACKNOWLEDGMENTS

We thank Lawrence Uricchio and David Enard for advice, discussions, and Tanya Phung, Jazlyn Mooney, Clare Marsden and Jesse Garcia for helpful comments on our manuscript. This work was supported by a Searle Scholars Fellowship and NIH Grant R35GM119856 (to K.E.L.) and foundation of Westlake University and NSFC 31900315 (to Y.Z.). We acknowledge support from a QCB Collaboratory Postdoctoral Fellowship to Y.Z. and the QCB Collaboratory Community directed by Matteo Pellegrini.

Author contributions

K.E.L conceived of and supervised the study. Y.Z. carried out all analyses on positive selection and generated all figures. C.D.H carried demographic and gamma-DFE inference. R.W.D. processed mice raw data to genotypes. Y.Z., C.D.H., R.W.D and K.E.L. all participated in manuscript preparation.

DISCLOSURE DECLARATION

The authors declare no competing interests.

REFERENCES

Andolfatto P. 2005. Adaptive evolution of non-coding DNA in Drosophila. *Nature* **437**: 1149–1152.

Andolfatto P, Wong KM, Bachtrog D. 2011. Effective population size and the efficacy of selection on the X chromosomes of two closely related Drosophila species. *Genome Biol Evol* **3**: 114–128.

Bolívar P, Mugal CF, Nater A, Ellegren H. 2015. Recombination rate variation modulates gene sequence evolution mainly via GC-biased gene conversion, not Hill–Robertson interference, in an avian system. *Mol Biol Evol* msv214.

685 Booker TR. 2019. Inferring parameters of the distribution of fitness effects of new
686 mutations when beneficial mutations are strongly advantageous and rare. *bioRxiv*
687 855411.

688 Booker TR, Keightley PD. 2018. Understanding the factors that shape patterns of nucleotide
689 diversity in the house mouse genome. *Mol Biol Evol* **35**: 2971–2988.

690 Boyko AR, Williamson SH, Indap AR, Degenhardt JD, Hernandez RD, Lohmueller KE, Adams
691 MD, Schmidt S, Sninsky JJ, Sunyaev SR, et al. 2008. Assessing the evolutionary impact
692 of amino acid mutations in the human genome. *PLoS Genet* **4**: e1000083.

693 Burgess R, Yang Z. 2008. Estimation of hominoid ancestral population sizes under bayesian
694 coalescent models incorporating mutation rate variation and sequencing errors. *Mol*
695 *Biol Evol* **25**: 1979–1994.

696 Bustamante CD, Fledel-Alon A, Williamson S, Nielsen R, Hubisz MT, Glanowski S,
697 Tanenbaum DM, White TJ, Sninsky JJ, Hernandez RD, et al. 2005. Natural selection
698 on protein-coding genes in the human genome. *Nature* **437**: 1153–1157.

699 Campos JL, Zhao L, Charlesworth B. 2017. Estimating the parameters of background
700 selection and selective sweeps in Drosophila in the presence of gene conversion.
701 *Proc Natl Acad Sci* **114**: E4762–E4771.

702 Charlesworth J, Eyre-Walker A. 2008. The McDonald–Kreitman test and xlightly deleterious
703 mutations. *Mol Biol Evol* **25**: 1007–1015.

704 Chen F-C, Li W-H. 2001. Genomic divergences between humans and other hominoids and
705 the effective population size of the common ancestor of humans and chimpanzees.
706 *Am J Hum Genet* **68**: 444–456.

707 Connallon T, Clark AG. 2015. The distribution of fitness effects in an uncertain world. *Evol*
708 *Int J Org Evol* **69**: 1610–1618.

709 The 1000 Genomes Project Consortium. 2012. An integrated map of genetic variation from
710 1,092 human genomes. *Nature* **491**: 56–65.

711 Corbett-Detig RB, Hartl DL, Sackton TB. 2015. Natural selection constrains neutral diversity
712 across a wide range of species. *PLoS Biol* **13**: e1002112.

713 Corcoran P, Gossmann TI, Barton HJ, Slate J, Zeng K. 2017. Determinants of the efficacy of
714 natural selection on coding and noncoding variability in two passerine species.
715 *Genome Biol Evol* **9**: 2987–3007.

716 Duncan BK, Miller JH. 1980. Mutagenic deamination of cytosine residues in DNA. *Nature*
717 **287**: 560.

718 Duret L, Galtier N. 2009. Biased Gene Conversion and the Evolution of Mammalian Genomic
719 Landscapes. *Annu Rev Genomics Hum Genet* **10**: 285–311.

720 Elyashiv E, Sattath S, Hu TT, Strutsovsky A, McVicker G, Andolfatto P, Coop G, Sella G. 2016.
721 A genomic map of the effects of linked selection in Drosophila. *PLOS Genet* **12**:
722 e1006130.

723 Enard D, Messer PW, Petrov DA. 2014. Genome-wide signals of positive selection in human
724 evolution. *Genome Res* **24**: 885–895.

725 Eyre-Walker A. 2002. Changing effective population size and the McDonald-Kreitman test.
726 *Genetics* **162**: 2017–2024.

727 Eyre-Walker A, Keightley PD. 2009. Estimating the rate of adaptive molecular evolution in
728 the presence of slightly deleterious mutations and population size change. *Mol Biol*
729 *Evol* **26**: 2097–2108.

730 Fay JC. 2011. Weighing the evidence for adaptation at the molecular level. *Trends Genet* **27**:
731 343–349.

732 Fay JC, Wyckoff GJ, Wu CI. 2001. Positive and negative selection on the human genome.
733 *Genetics* **158**: 1227–1234.

734 Fay JC, Wyckoff GJ, Wu C-I. 2002. Testing the neutral theory of molecular evolution with
735 genomic data from Drosophila. *Nature* **415**: 1024–1026.

736 Fischer A, Wiebe V, Pääbo S, Przeworski M. 2004. Evidence for a complex demographic
737 history of chimpanzees. *Mol Biol Evol* **21**: 799–808.

738 Foxe JP, Dar V-N, Zheng H, Nordborg M, Gaut BS, Wright SI. 2008. Selection on amino acid
739 substitutions in Arabidopsis. *Mol Biol Evol* **25**: 1375–1383.

740 Galtier N. 2016. Adaptive Protein evolution in animals and the effective population size
741 hypothesis. *PLoS Genet* **12**: e1005774.

742 Gillespie JH. 2004. Why k=4Nus is silly. In *The Evolution of Population Biology*. (ed. RS Singh
743 and MK Uyenoyama), pp. 178-192. Cambridge University Press, Cambridge, UK.

744 Gossmann TI, Keightley PD, Eyre-Walker A. 2012. The effect of variation in the effective
745 population size on the rate of adaptive molecular evolution in eukaryotes. *Genome*
746 *Biol Evol* **4**: 658–667.

747 Gossmann TI, Song B-H, Windsor AJ, Mitchell-Olds T, Dixon CJ, Kapralov MV, Filatov DA,
748 Eyre-Walker A. 2010. Genome wide analyses reveal little evidence for adaptive
749 evolution in many plant species. *Mol Biol Evol* **27**: 1822–1832.

750 Halligan DL, Kousathanas A, Ness RW, Harr B, Eöry L, Keane TM, Adams DJ, Keightley PD.
751 2013. Contributions of protein-coding and regulatory change to adaptive molecular
752 evolution in murid rodents. *PLoS Genet* **9**: e1003995.

753 Halligan DL, Oliver F, Eyre-Walker A, Harr B, Keightley PD. 2010. Evidence for pervasive
754 adaptive protein evolution in wild mice. *PLoS Genet* **6**: e1000825.

755 Hernandez RD, Hubisz MJ, Wheeler DA, Smith DG, Ferguson B, Rogers J, Nazareth L, Indap
756 A, Bourquin T, McPherson J, et al. 2007. Demographic histories and patterns of
757 linkage disequilibrium in Chinese and Indian rhesus macaques. *Science* **316**: 240–
758 243.

759 Hobolth A, Christensen OF, Mailund T, Schierup MH. 2007. Genomic relationships and
760 speciation times of human, chimpanzee, and gorilla inferred from a coalescent
761 hidden Markov model. *PLoS Genet* **3**: e7.

762 Hu TT, Eisen MB, Thornton KR, Andolfatto P. 2013. A second-generation assembly of the
763 Drosophila simulans genome provides new insights into patterns of lineage-specific
764 divergence. *Genome Res* **23**: 89–98.

765 Huber CD, Kim BY, Marsden CD, Lohmueller KE. 2017. Determining the factors driving
766 selective effects of new nonsynonymous mutations. *Proc Natl Acad Sci* **114**: 4465–
767 4470.

768 Hvilsom C, Qian Y, Bataillon T, Li Y, Mailund T, Sallé B, Carlsen F, Li R, Zheng H, Jiang T, et al.
769 2012. Extensive X-linked adaptive evolution in central chimpanzees. *Proc Natl Acad*
770 *Sci* **109**: 2054–2059.

771 Keightley PD, Campos JL, Booker TR, Charlesworth B. 2016. Inferring the frequency
772 spectrum of derived variants to quantify adaptive molecular evolution in protein-
773 coding genes of Drosophila melanogaster. *Genetics* **203**: 975–984.

774 Kimura M. 1962. On the probability of fixation of mutant genes in a population. *Genetics* **47**:
775 713–719.

776 Kimura M. 1983. *The Neutral Theory of Molecular Evolution*. Cambridge University Press,
777 Cambridge.

778 Lachance J, Tishkoff SA. 2014. Biased gene conversion skews allele frequencies in human
779 populations, increasing the disease burden of recessive alleles. *Am J Hum Genet* **95**:
780 408–420.

781 Lack JB, Cardeno CM, Crepeau MW, Taylor W, Corbett-Detig RB, Stevens KA, Langley CH,
782 Pool JE. 2015. The Drosophila Genome Nexus: A population genomic resource of 623
783 *Drosophila melanogaster* genomes, including 197 from a single ancestral range
784 population. *Genetics* **199**: 1229–1241.

785 Li H, Durbin R. 2009. Fast and accurate short read alignment with Burrows-Wheeler
786 transform. *Bioinforma Oxf Engl* **25**: 1754–1760.

787 Lourenço JM, Glémin S, Galtier N. 2013. The rate of molecular adaptation in a changing
788 environment. *Mol Biol Evol* **30**: 1292–1301.

789 Lunter G, Goodson M. 2011. Stampy: a statistical algorithm for sensitive and fast mapping
790 of Illumina sequence reads. *Genome Res* **21**: 936–939.

791 McDonald JH, Kreitman M. 1991. Adaptive protein evolution at the Adh locus in Drosophila.
792 *Nature* **351**: 652–654.

793 McKenna A, Hanna M, Banks E, Sivachenko A, Cibulskis K, Kernytsky A, Garimella K,
794 Altshuler D, Gabriel S, Daly M, et al. 2010. The Genome Analysis Toolkit: a
795 MapReduce framework for analyzing next-generation DNA sequencing data. *Genome*
796 *Res* **20**: 1297–1303.

797 McVicker G, Gordon D, Davis C, Green P. 2009. Widespread genomic signatures of natural
798 selection in hominid evolution. *PLoS Genet* **5**: e1000471.

799 Messer PW, Petrov DA. 2013. Frequent adaptation and the McDonald–Kreitman test. *Proc*
800 *Natl Acad Sci* **110**: 8615–8620.

801 Nam K, Munch K, Mailund T, Nater A, Greminger MP, Krützen M, Marquès-Bonet T,
802 Schierup MH. 2017. Evidence that the rate of strong selective sweeps increases with
803 population size in the great apes. *Proc Natl Acad Sci U S A* **114**: 1613–1618.

804 Ness RW, Zhang Y-H, Cong L, Wang Y, Zhang J-X, Keightley PD. 2012. Nuclear gene variation
805 in wild brown rats. *G3 Genes Genomes Genet* **2**: 1661–1664.

806 Ohta T. 1973. Slightly deleterious mutant substitutions in evolution. *Nature* **246**: 96–98.

807 Ohta T. 1992. The nearly neutral theory of molecular evolution. *Annu Rev Ecol Syst* **23**: 263–
808 286.

809 Orr HA. 1998. The population genetics of adaptation: The distribution of factors fixed
810 during adaptive evolution. *Evolution* **52**: 935–949.

811 Phifer-Rixey M, Bonhomme F, Boursot P, Churchill GA, Piálek J, Tucker PK, Nachman MW.
812 2012. Adaptive evolution and effective population size in wild house mice. *Mol Biol*
813 *Evol* **29**: 2949–2955.

814 Prado-Martinez J, Sudmant PH, Kidd JM, Li H, Kelley JL, Lorente-Galdos B, Veeramah KR,
815 Woerner AE, O'Connor TD, Santpere G, et al. 2013. Great ape genetic diversity and
816 population history. *Nature* **499**: 471–475.

817 Pritchard JK, Pickrell JK, Coop G. 2010. The genetics of human adaptation: hard sweeps, soft
818 sweeps, and polygenic adaptation. *Curr Biol* **20**: R208–R215.

819 Robinson MC, Stone EA, Singh ND. 2014. Population genomic analysis reveals no evidence
820 for GC-biased gene conversion in *Drosophila melanogaster*. *Mol Biol Evol* **31**: 425–
821 433.

822 Romiguier J, Gayral P, Ballenghien M, Bernard A, Cahais V, Chenuil A, Chiari Y, Dernat R,
823 Duret L, Faivre N, et al. 2014. Comparative population genomics in animals uncovers
824 the determinants of genetic diversity. *Nature* **515**: 261–263.

825 Rousselle M, Mollion M, Nabholz B, Bataillon T, Galtier N. 2018. Overestimation of the
826 adaptive substitution rate in fluctuating populations. *Biol Lett* **14**: 20180055.

827 Rousselle M, Simion P, Tilak MK, Figuet E, Nabholz B, Galtier N. 2019. Is adaptation limited
828 by mutation? A timescale-dependent effect of genetic diversity on the adaptive
829 substitution rate in animals. *bioRxiv* 643619.

830 Sawyer SA, Hartl DL. 1992. Population genetics of polymorphism and divergence. *Genetics*
831 **132**: 1161–1176.

832 Schneider A, Charlesworth B, Eyre-Walker A, Keightley PD. 2011. A method for inferring
833 the rate of occurrence and fitness effects of advantageous mutations. *Genetics* **189**:
834 1427–1437.

835 Schrago CG. 2014. The effective population sizes of the anthropoid ancestors of the human–
836 chimpanzee lineage provide insights on the historical biogeography of the great
837 apes. *Mol Biol Evol* **31**: 37–47.

838 Sella G, Petrov DA, Przeworski M, Andolfatto P. 2009. Pervasive natural selection in the
839 Drosophila genome? *PLoS Genet* **5**: e1000495.

840 Smith NGC, Eyre-Walker A. 2002. Adaptive protein evolution in Drosophila. *Nature* **415**:
841 1022–1024.

842 Strasburg JL, Kane NC, Raduski AR, Bonin A, Michelmore R, Rieseberg LH. 2011. Effective
843 population size is positively correlated with levels of adaptive divergence among
844 annual sunflowers. *Mol Biol Evol* **28**: 1569–1580.

845 Stumpf MPH, Thorne T, Silva E de, Stewart R, An HJ, Lappe M, Wiuf C. 2008. Estimating the
846 size of the human interactome. *Proc Natl Acad Sci* **105**: 6959–6964.

847 Sved J, Bird A. 1990. The expected equilibrium of the CpG dinucleotide in vertebrate
848 genomes under a mutation model. *Proc Natl Acad Sci U S A* **87**: 4692–4696.

849 Tataru P, Mollion M, Glémin S, Bataillon T. 2017. Inference of distribution of fitness effects
850 and proportion of adaptive substitutions from polymorphism data. *Genetics* **207**:
851 1103–1119.

852 Torgerson DG, Boyko AR, Hernandez RD, Indap A, Hu X, White TJ, Sninsky JJ, Cargill M,
853 Adams MD, Bustamante CD, et al. 2009. Evolutionary processes acting on candidate
854 cis-regulatory regions in humans inferred from patterns of polymorphism and
855 divergence. *PLoS Genet* **5**: e1000592.

856 Uricchio LH, Petrov DA, Enard D. 2019. Exploiting selection at linked sites to infer the rate
857 and strength of adaptation. *Nat Ecol Evol* **3**: 977–984.

858 Valentine JW, Collins AG, Meyer CP. 1994. Morphological complexity increase in metazoans.
859 *Paleobiology* **20**: 131–142.

860 Veeramah KR, Gutenkunst RN, Woerner AE, Watkins JC, Hammer MF. 2014. Evidence for
861 increased levels of positive and negative selection on the X chromosome versus
862 autosomes in humans. *Mol Biol Evol* **31**: 2267–2282.

863 Wall JD. 2013. Great Ape Genomics. *ILAR J* **54**: 82–90.

864 Xue C, Raveendran M, Harris RA, Fawcett GL, Liu X, White S, Dahdouli M, Rio Deiros D,
865 Below JE, Salerno W, et al. 2016. The population genomics of rhesus macaques
866 (Macaca mulatta) based on whole-genome sequences. *Genome Res* **26**: 1651–1662.

867 Yang H, Ding Y, Hutchins LN, Szatkiewicz J, Bell TA, Paigen BJ, Graber JH, de Villena FP-M,
868 Churchill GA. 2009. A customized and versatile high-density genotyping array for
869 the mouse. *Nat Methods* **6**: 663–666.

870

871
872

873 Table 1. Estimates of α using different methods

			Method of Inference					
	Species	Outgroup	MK-method: all	MK-method: MAF>20%	Model-based: Simple Model	Model-based: Complex Model	DFEα: α	DFEα: omega_a
Full data	Human	Chimpanzee	-0.41	-0.01	0.11	0.25	0.24	0.07
	Human	Macaque	-0.70	-0.22	-0.08	0.26	0.02	0.01
	Human lineage	-	-	-	0.06	0.16	-	-
	D. melanogaster	*D. simulans*	-0.13	0.49	0.53	0.60	0.71	0.14
	Mice	Rat	0.25	0.40	0.45	0.41	0.51	0.12
SSWW only	Human	Chimpanzee	-0.37	0.08	0.13	0.26	-	-
	Mice	Rat	-0.14	0.08	0.20	0.10	-	-

874

875

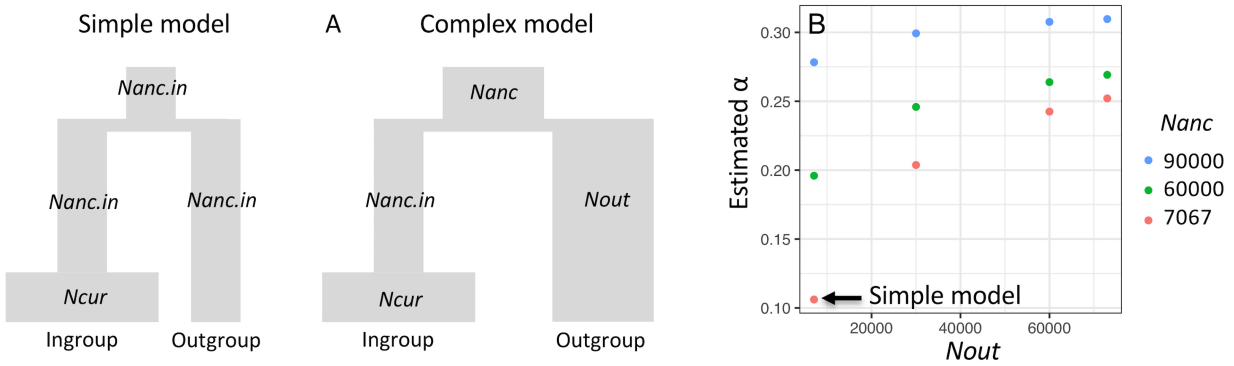

Figure 1. The ancestral and outgroup population sizes greatly influence α. (A). Schematic demographic models illustrate the Simple and the Complex model with associated parameters. In the Simple model, the size of the ancestral population (*Nanc)* as well as the size of the outgroup (*Nout*) are assumed to be the same as the ancestral size of the ingroup (*Nanc.in*). This assumption is relaxed in the Complex model. (B). Effect of *Nanc* and *Nout* on estimates of α for humans using the chimpanzee as an outgroup. Colors denote different values of *Nanc*. Arrow points to the estimate of α from the Simple model where *Nanc* = *Nout* = *Nanc.in* = 7067.

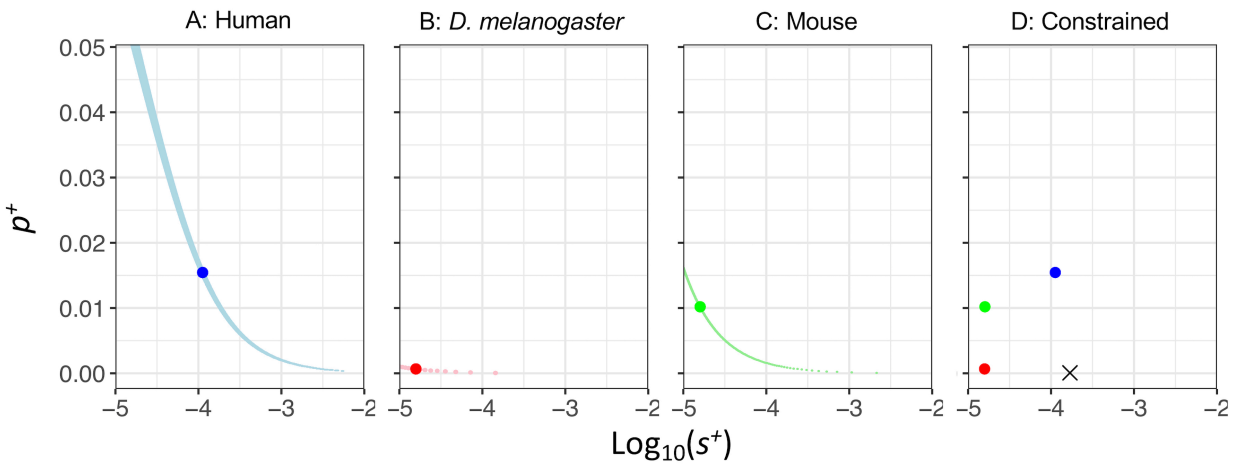

Figure 2. Log-likelihood surfaces for p^+ and s^+ for different species. (A) Human. (B) *D. melanogaster*. (C) Mouse. (D) The constrained model (H0), where p^+ and s^+ are constrained to be the same across all three taxa. Log-Likelihoods (LL) are calculated using grid search method of $\log_{10}(s^+)$ in the range of -5 to -2 and p^+ in the range of 0-7.5%. Blue denotes human, red denotes *D. melanogaster*, and green denotes mouse. The large points represent the MLE for each species, the black cross in panel D represents the MLE of the constrained model, and the lighter colors show grid points within 3 LL units of each MLE. The Complex model is used for each species and we use the chimpanzee as the outgroup for humans.

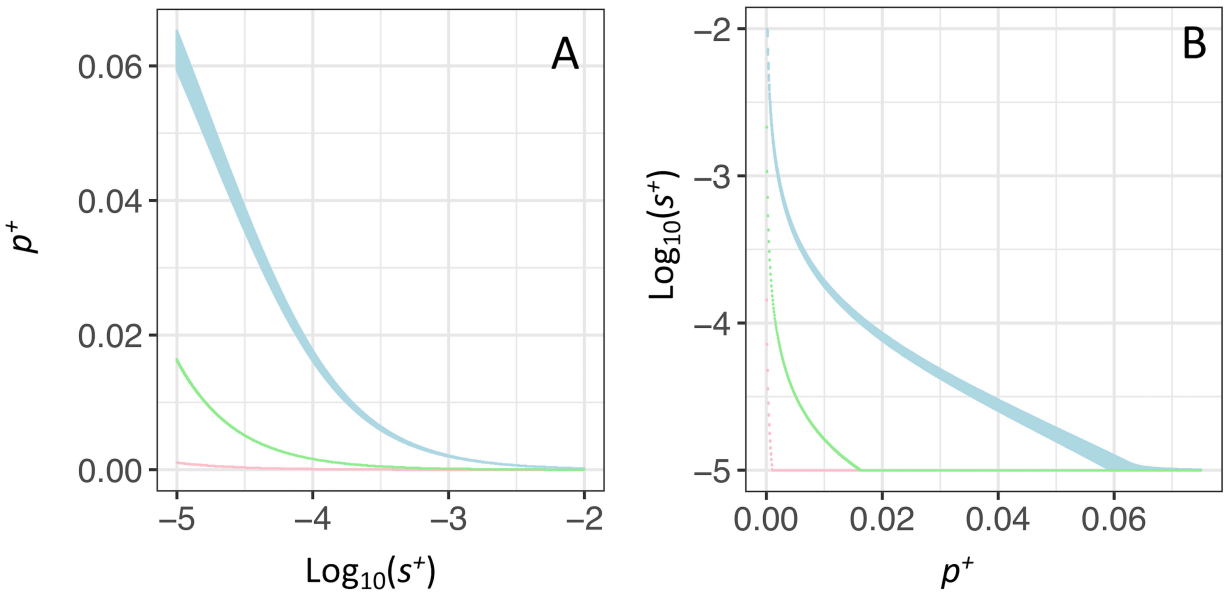

Figure 3. Conditional log-likelihood surfaces. (A) Maximizing p^+ given particular values of s^+ and (B) maximizing s^+ given particular values of p^+. Only grid points within 3 LL units of the MLEs for each parameter for each species are shown. Light blue denotes human, pink denotes *D. melanogaster*, and light green denotes mouse.

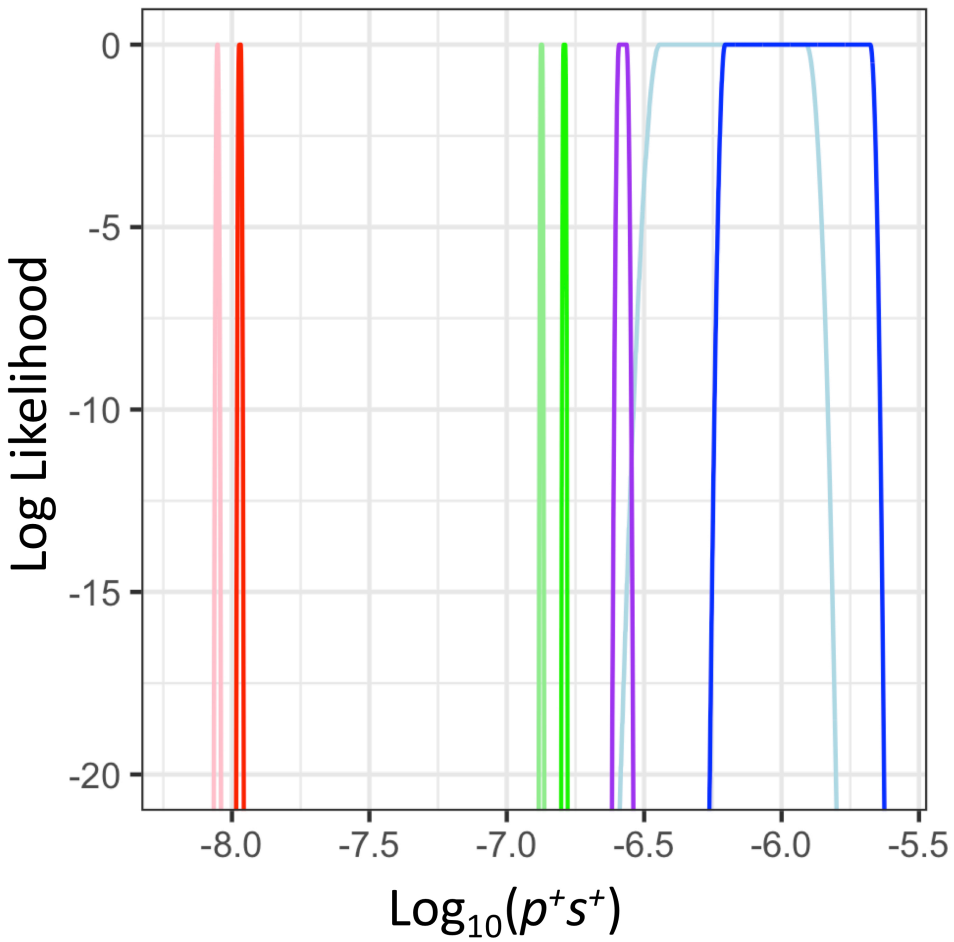

Figure 4. The composite parameter $p^{+}s^{+}$, capturing the proportion of beneficial mutations and the strength of selection, differs across species. Log-likelihood curves for $p^{+}s^{+}$ in the three species. Red denotes the inference for *D. melanogaster*, green denotes the inference for mouse, blue denotes the inference for human using the chimpanzee as the outgroup, and purple denotes the inference for human using the macaque as the outgroup. Lighter colors denote the Simple model. Darker colors denote the Complex model that better models the ancestral demography and population size of the outgroup. Note that regardless of which demographic model is used, the log-likelihood curves from the different species do not overlap within the top 500 log-likelihood units, suggesting $p^{+}s^{+}$ is significantly different among taxa.

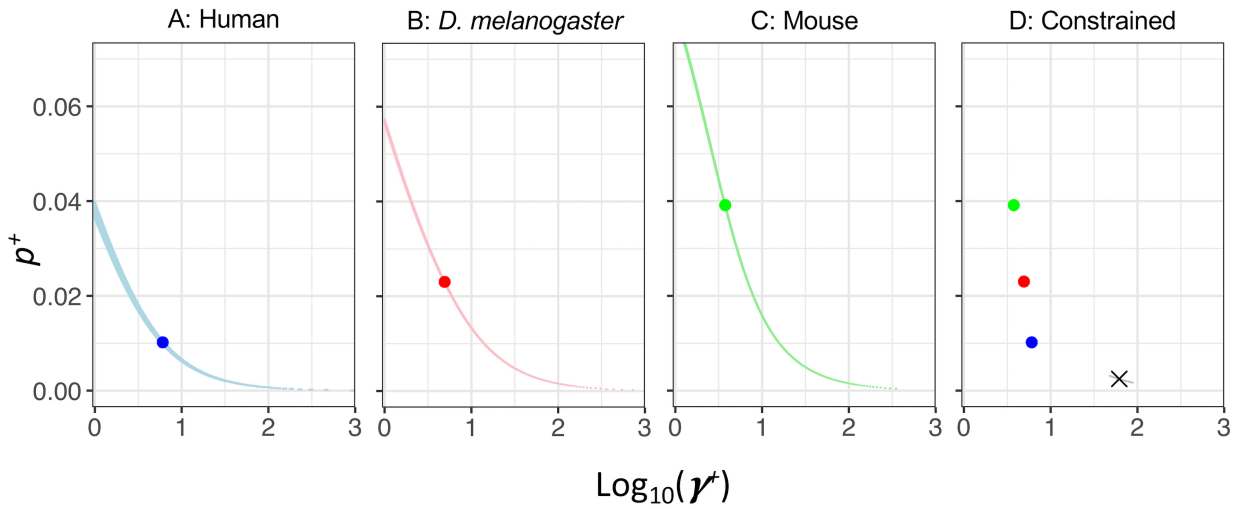

Figure 5. Log-likelihood surfaces for p^+ and γ^+ for different species. (A) Human. (B) *D. melanogaster*. (C) Mouse. (D) The constrained model, H0, where p^+ and γ^+ are constrained to be the same across all three taxa. Log-likelihoods are calculated using grid search method of $\log_{10}(\gamma^+)$ in the range of 0-3 and p^+ in the range of 0-7.5%. Blue denotes human, red denotes *D. melanogaster*, and green denotes mouse. The large points represent the MLE for each species, the black cross in panel D represents the MLE of the constrained model, and the lighter colors show grid points within 3 LL units of each MLE. The Complex model is used for each species and we use chimpanzee as the outgroup for humans.